Front. Phys. China (2006) 4: 458－467
DOI 10.1007/s11467-006-0047-3

REVIEW ARTICLE

ZHENG Zhi-gang , FENG Xiao-qin, AO Bin, Michael C. Cross

Synchronization on coupled dynamical networks

Abstract In this paper, partial synchronization (PaS) in networks of coupled chaotic oscillator systems and synchronization in sparsely coupled spatiotemporal systems are explored. For the PaS, we reveal that the existence of PaS patterns depends on the symmetry property of the network topology, while the emergence of the PaS pattern depends crucially on the stability of the corresponding solution. An analytical criterion in judging the stability of PaS state on a given network are proposed in terms of a comparison between the Lyapunov exponent spectrum of the PaS manifold and that of the transversal manifold. The competition and selections of the PaS patterns induced by the presence of multiple topological symmetries of the network are studied in terms of the criterion. The phase diagram in distinguishing the synchronous and the asynchronous states is given. The criterion in judging PaS is further applied to the study of synchronization of two sparsely coupled spatiotemporal chaotic systems. Different synchronization regimes are distinguished. The present study reveals the intrinsic collective bifurcation of coupled dynamical systems prior to the emergence of global synchronization.

Keywords complex networks, synchronization, partial synchronization, chaos

PACS numbers 05.45.-a, 82.40.Bj

ZHENG Zhi-gang (✉), FENG Xiao-qin
Department of Physics and the Beijing-Hong Kong-Singapore Joint Center for Nonlinear and Complex Systems (Beijing), Beijing Normal University, Beijing 100875, China
E-mail: zgzheng@bnu.edu.cn

AO Bin
Center for Nonlinear Studies and Department of Physics, Hong Kong Baptist University, Hong Kong, China

Michael C. Cross
Department of Physics, California Institute of Technology, Pasadena 91125, USA

Received September 19, 2006

1 Introduction

Synchronization is one of the simplest types of collective dynamics among coupled dynamical systems, and synchronization phenomenon occurs ubiquitously in physics, chemistry, and biology [1－5, 12－16]. Synchronous dynamics of chaotic motions received much attention due to its intuitive controversy with the usual concept of chaotic motion (the well known butterfly effect, i.e., the exponential divergence of small deviation of chaotic orbit) and complicated manifestations. Since the work of Pecora and Carroll on complete synchronization [1－5], different types of chaos synchronizations, such as generalized synchronization (GS) [6－11], phase synchronization (PS) [12] and partial synchronization (PaS) [13－15] have been revealed and exhaustively investigated.

Complex networks have attracted considerable research interest in recent years [17－20]. The problems that are mainly focused on are the topological features of these diverse networks and the effect of topological structures on the dynamics. When a group of oscillators are coupled to each other to form a network, e.g., the small-world networks, scale-free networks, and so on, various topological features of network such as the average shortest path, clustering coefficient, the degree distribution, and so on, can strongly affect the synchronizability of the dynamics network [21－32]. However, due to the complexity of the networks, the dominant ingredient that determines the synchronization in coupled chaotic oscillator networks is still not clear, and the dependence of synchronizability on the network topology had given rise to a number of disputes.

There have been numerous studies on the dynamics of global synchronization on complex networks. To simplify the investigation, it is instructive to study the collective dy namics of a regular network with only a few nonlocal couplings, which is much simpler than diverse cases that have been explored before. Shortcuts have been revealed to play a very important role in governing the synchronous dynamics on networks [33]. By considering one or two nonlocal links, one may systematically study the effect of adding shortcuts

on synchronization. As will shown in this paper, even when we add only one or two shortcuts, different ways of nonlocal links may strongly influence the collective dynamics. More interestingly, we can observe an interesting partially synchronous state.

PaS of chaotic oscillators has been extensively investigated in globally coupled systems, where no space structure can be involved [34]. PaS in locally coupled systems has been also revealed [35]. The existence of the PaS solution on arbitrary networks has been discussed by using symmetry analysis of the network topology [36]. In realistic situations, the observability of the PaS state depends crucially on the stability of the PaS solution. It should be very important to propose a theoretical criterion for the stability of the PaS solution. It would also be significant to study the effect of the way of adding a few shortcuts on a regular network on the PaS patterns by using the criterion. This may open a new idea in controlling the patterns by adjusting the topology of the network.

In this paper, we reveal the partial synchronization (PaS) phenomena on irregular networks. Various synchronous patterns are observed for different types of networks. This reveals the significant role of network topology in governing the global dynamics. We analyze in detail the conditions for the emergence of the PaS and give the criterion of the topological dependence of the stability of the PaS. The PaS dynamics on various networks with a few shortcuts are explored in terms of the theoretical criterion, and the synchronous phase diagram is given [37−40]. The analytical criterion we proposed for PaS can be well extended to the synchronization of sparsely coupled spatiotemporal systems [41], and the relation between the synchronizability and the ways of intergroup links is revealed.

2 Partial synchronization: phenomena

Let us start with N m-dimensional nonlinear oscillators with individual dynamics:

$$\dot{\boldsymbol{x}} = \boldsymbol{f}(\boldsymbol{x}), \quad \boldsymbol{x} = (x_1, x_2, \cdots, x_m) \tag{1}$$

When these oscillators are coupled to each other in a certain way, we can regard individual oscillators as the nodes, and the couplings among these oscillators as the edges. The equations of motion in governing the dynamics of such a network can be described by:

$$\dot{\boldsymbol{x}} = \boldsymbol{F}(\boldsymbol{X}) + \varepsilon \Gamma \otimes C\boldsymbol{X} \tag{2}$$

where $\boldsymbol{X} = (\boldsymbol{x}^1, \boldsymbol{x}^2, \cdots, \boldsymbol{x}^N)$, $\boldsymbol{F} = (\boldsymbol{f}^1, \boldsymbol{f}^2, \cdots, \boldsymbol{f}^N)$, and N is the number of nodes. The second term in Eq. (2) represents the coupling (edges) among oscillators (nodes). ε denotes the coupling strength, and $\Gamma : \mathbb{R}^m \to \mathbb{R}^m$ characterizes the coupling scheme among the nodes. $C = M–D$, where M is the adjacency matrix of the network (the element M_{ij} denotes the number of edges that link nodes i and j), and D is a diagonal matrix with diagonal elements $D_{ii} = \sum_{j=1}^{N} M_{ij}$. Therefore $\sum_{j=1}^{N} C_{ij} = 0$, and its largest eigenvalue $\lambda_1^C = 0$. We adopt

$$\lambda_1 \geqslant \lambda_2 \geqslant \cdots \geqslant \lambda_N \tag{3}$$

throughout this paper unless specifically mentioned.

We are interested in the collective dynamics of the system when the globally synchronous state is unstable (2). The synchronization between two oscillators i and j can conveniently measured by introducing the average distance $d_{ij} = \lim_{T\to\infty}(T^{-1}\int \| \boldsymbol{x}_i - \boldsymbol{x}_j \| \mathrm{d}t)$, where $\| \bullet \|$ denotes the Euclidian distance, and T is the temporal integral interval. Two oscillators are in the synchronous state in the sense that $d_{ij} = 0$.

We take a ten-node-ring network with one non-local coupling [e.g., node 1 links to node 4, denoted by (1, 4)] as our first example to reveal the PaS phenomenon, as shown schematically in Fig. 1 (a). We choose the Lorenz oscillator [$\dot{x} = \sigma(y - x)$, $\dot{y} = \gamma x - y - xz$, $\dot{z} = xy - \beta z$] as our nodes. Parameters are chosen as $\sigma = 10$, $\gamma = 27$, $\beta = 8/3$, where the dynamics of individual node is chaotic. The coupling scheme is adopted as:

$$\Gamma = \begin{pmatrix} 0 & 0 & 0 \\ 1 & 0 & 0 \\ 0 & 0 & 0 \end{pmatrix}$$

In Fig. 1 (b), the distances between two oscillators $d_{1,2}$, $d_{1,10}$, $d_{2,9}$, $d_{3,8}$ and $d_{4,7}$ against the coupling strength ε are computed. It can be found that for two oscillators 1 and 4, which are coupled with one nonlocal link, $d_{1,4} \to 0$ at $\varepsilon_1 = 6.6$, while for two oscillators 1 and 2 that are also locally coupled to each other, $d_{1,2} \to 0$ at a much larger critical coupling strength $\varepsilon_2 = 23.4$. This phenomenon is very interesting because some nearest-neighbor coupled oscillators (e.g., No.1 and 4) on this network can be synchronized to each other at this weak coupling, while others (e.g., No.1 and 2) cannot achieve the synchronous state at this weak coupling. Moreover, we find that $d_{2,3}$, $d_{1,4}$, $d_{5,10}$, $d_{6,9}$, $d_{2,3}$ and $d_{7,8}$ become 0 at ε_1, i.e., oscillators form some synchronized clusters. We call the emergence of synchronized clusters the *partial synchronization* (PaS). It is interesting to find from Fig. 1 that partial synchronization also emerges among oscillators that aren't linked directly, e.g. $d_{5,10} = 0$ and $d_{6,9} = 0$ at $\varepsilon = \varepsilon_1$ in Fig. 1 (b). It is interesting that these synchronized clusters are formed at the same critical coupling. In Fig. 1 (a), the same symbols denote oscillators in one synchronous cluster. As shown in Fig. 1 (a), the network are divided into $N/2 = 5$ clusters. We also found that the emergence of the PaS is irrelevant to the node dynamics and the number of oscillators.

Different topologies of adding non-local couplings may lead to different PaS patterns and moreover different numbers of synchronous clusters. Figure 2 (a) gives the case of $N = 10$ with one (1, 5) shortcut. Six different clusters can be observed, and some clusters only include one node. By com-

paring the above two cases, one can find that synchronization always emerges between nodes with the mirror symmetry of the lattice (clearly labelled by the symmetry axis with a dashed line). Figures 2 (b)—(d) give some different types of networks with mirror symmetry. One can also observe the PaS phenomena.

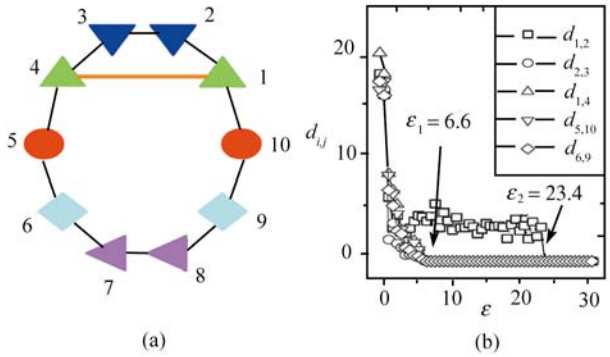

Fig. 1 **(a)** The topological graph of networks with 10 nodes and a nonlocal coupling between node 1 and node 4 denoted by (1,4). **(b)** The relationship between the average distance and the coupling strength on the network in which the Lorenz oscillator is adopted as nodes.

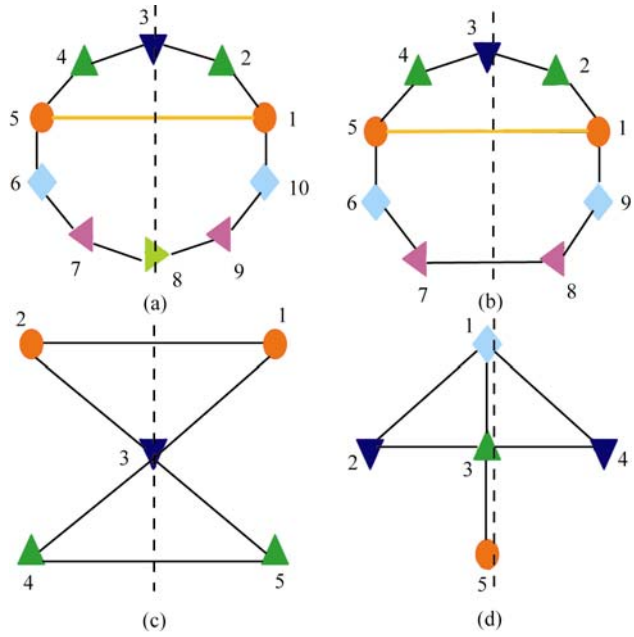

Fig. 2 The topological graphs of networks with different topological structures. **(a)** $N = 10$, (1, 5) being the shortcut, six synchronized clusters can be observed. **(b)** $N = 9$, (1, 5) being the shortcut, five synchronous clusters are observed. **(c)** A network with two symmetrical axis network (labelled by dashed and dotted lines ,and PaS can be observed in one of these two symmetric cases. **(d)** Another network that can achieve the PaS, its symmetry axis coincides with one of its edges

Our numerical simulations reveal that PaS can always be achieved on a ring network with one non-local coupling (denoted by $N_s = 1$), and these networks always have the mirror symmetry. However, for networks with more shortcuts, e. g., $N_s = 2$, the results become more complicated. PaS can't be achieved in the network shown in Fig. 3 (a), because one cannot find any symmetry of the network. These results indicate that the existence of topological symmetry of a network is the necessary condition for the emergence of the PaS. In fact, from a theoretical point of view, the emergence of synchronization among oscillators requires the dynamics (the form of the equations, particularly including the form of the couplings) of each oscillator within a synchronous cluster are the same [44]. This can never be satisfied on a network without any symmetry. The networks shown in Figs. 3 (b), (c) and (d) have the mirror symmetry, and hence it is possible to observe the PaS phenomena on these networks.

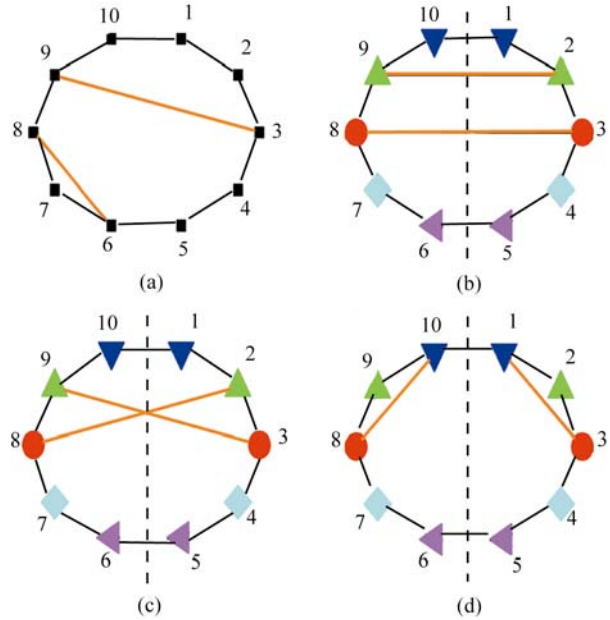

Fig. 3 The topological graph of the ring network with two nonlocal couplings. **(a)** A network without any topological symmetry. **(b)** The "paral-Lel" network with two parallel shortcuts. **(c)** The "cross" network with two crossing nonlocal couplings. **(d)** The "lambda" network, where two shortcuts are neither crossing nor parallel to each other.

A natural question arises: while the network symmetry is the necessary condition for the emergence of PaS, can PaS always be achieved on a network with a symmetry ? The answer is "No". As shown in Figs. 4 (a) and (b), these network topologies also possess the mirror symmetry respectively, but PaS can't be observed. Therefore it is interesting to study what kind of network topology can have a stable PaS pattern. Another interesting while important issue is related to networks with multiple topological symmetries. Can PaS also be achieved on a network with more than one symmetry ? Which symmetry can dominate the emergence of the PaS ? As an example, for the network shown in Fig. 4 (c) [$N = 8$, $N_s = 2$, (1, 5), (3, 7)], there are three rotation symmetries and four mirror symmetries, but PaS can not be observed on this network. However, for the network shown in Fig. 2 (c), there are two mirror-symmetry axes, but only one of them determines the PaS pattern.

These exhaustive numerical results show us rich PaS pat-

terns and furthermore provide us a number of interesting questions. We find the emergence (formation) of PaS patterns due to the presence of some topological symmetry of the network, and we also observe the significant PaS pattern competitions and selections due to the presence of multiple topological symmetries. It is possible to find PaS solutions in terms of the symmetry analysis, but it is more important and necessary to theoretically study the sufficient condition of theemergence of the PaS. This condition should give us the wayin judging the observability of the PaS pattern of a given network and further study a number of related issues that are of profound importance.

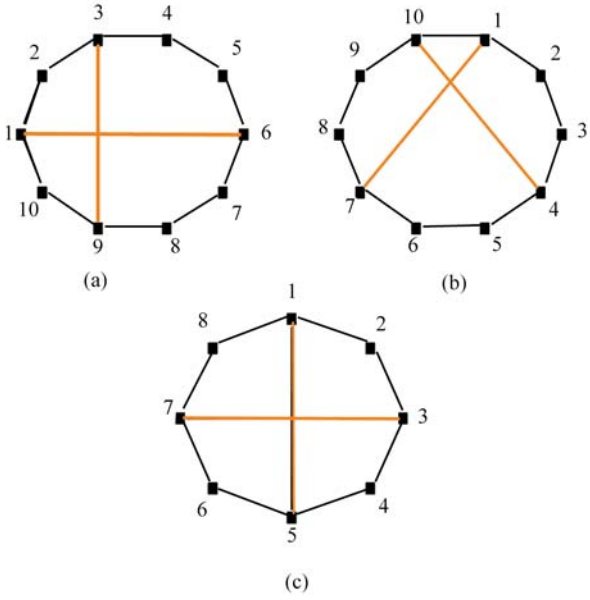

Fig. 4 Some examples of networks that have certain symmetry but can not possess an observable PaS state. **(a)** A "cross" network; **(b)** A "lambda" network; **(c)** An example that is compared with Fig. 3 (c), where the network has more than one symmetry, but PaS can the achieved.

3 The emergence of PaS: the criterion

In fact, according to the viewpoint of nonlinear dynamics, the PaS state should be a solution of Eq. (2), which can be described by:

$$\boldsymbol{x}_1^k = \boldsymbol{x}_2^k = \cdots = \boldsymbol{x}_{N_k}^k, \quad k = 1, 2, \cdots, N_c \tag{4}$$

where N_c is the number of PaS clusters, and N_k is the number of oscillators in the k-th synchronous cluster. Obviously one has the relation:

$$\sum_{k=1}^{N_c} N_k = N$$

These equations determine an mN_c-dimensional invariant submanifold. The symmetry of the network can only determine the existence of the synchronous solution or the PaS submanifold [36], while they cannot determine the stability of the PaS sub-manifold. To understand the stability of the PaS state, let us start with the theoretical analysis on the stability of the complete-synchronization (CS) manifold [42, 43].

3.1 Complete synchronization: The master stability function

For a differential dynamical system described by Eq. (2), if the globally synchronous state (solution):

$$\boldsymbol{x}^1(t) = \boldsymbol{x}^2(t) = \cdots = \boldsymbol{x}^N(t) = \boldsymbol{s}(t) \tag{5}$$

exists, one can linearize Eq. (2) in the vicinity of this synchronous manifold and analyze its stability. By inserting the perturbed solution $\boldsymbol{x}^i(t) = \boldsymbol{s}(t) + \boldsymbol{u}^i(t)$ $(i = 1, 2, \cdots, N)$ into C and linearizing it along the synchronous manifold $\boldsymbol{s}(t)$, one may get

$$\dot{\boldsymbol{U}}(t) = [\boldsymbol{I}_N \otimes D\boldsymbol{f}(\boldsymbol{s}) + \varepsilon \Gamma \otimes C]\, \boldsymbol{U}(t) \tag{6}$$

where $\boldsymbol{U} = (\boldsymbol{u}^1, \boldsymbol{u}^2, \cdots, \boldsymbol{u}^N)$ and $D\boldsymbol{f}$ is the Jacobian function of $\boldsymbol{f}$ near the synchronous state $\boldsymbol{s}(t)$. Noticing that the first term of Eq. (6) is block diagonal with $m \times m$ blocks, thus one can diagonalize the adjacent matrix C. By diagonalizing Eq. (2), one can decompose the linearized Eq. (6) into N independent eigen-modes:

$$\dot{\boldsymbol{v}}_k = [D\boldsymbol{f} + \varepsilon\lambda_k \Gamma]\, \boldsymbol{v}_k, \quad k = 1, 2, \cdots, N \tag{7}$$

where λ_k are eigenvalues of C. The stability of the complete-synchronization (CS) state is determined by looking for the regime where the largest Lyapunov exponent of the generic equation

$$\dot{\boldsymbol{v}} = [D\boldsymbol{f} + \alpha \Gamma]\, \boldsymbol{v} \tag{8}$$

is negative on the α plane (it should be noted that α can be complex). If all $\{\varepsilon\lambda_k\}$ $(k = 1, 2, \cdots, N)$ fall into the negative (stable) regime (except $\lambda_1 = 0$), then the CS state will be stable. The key point of this method is to decompose the dynamical system into two subsystems. One subsystem dominates the dynamics on the synchronous manifold described by the equations with λ_1=0, and the other describes the dynamics on the transversal manifold corresponding to the equations with λ_i $(i = 2, 3, \cdots, N)$. The emergence of the CS state is thus determined by the stability of the transversal system.

3.2 The adjacent matrix of a network

In fact, the above master stability function method can be well applied to the analysis of the stability of the PaS state. For the case of PaS, one also needs to decompose the system into two parts, and the stability of the transversal subsystem determines the emergence of the PaS. The PaS state we are studying in this paper satisfies the mirror symmetry. This makes the analytical treatment possible. Till now, to our knowledge, there has not been a theoretical criterion about

the presence of PaS. Therefore, a criterion in judging the partial synchronization should be significant.

The symmetry of a network can be defined by the invariance of its adjacent matrix C under a permutation transformation T, i.e.,

$$TCT^{-1} = C \tag{9}$$

For example, the permutation transformation T for the network shown in Fig. 2 (a) is

$$T = \begin{pmatrix} F_4 & 0_{4\times 6} \\ 0_{6\times 4} & F_6 \end{pmatrix} \tag{10}$$

where F_K is a $K\times K$ counteridentity matrix that satisfies $F_{i,K-i+1} = 1$, for $i = 1, 2, \cdots, K$ and $F_{ij} = 0$ for all $i+j \neq K/2+1$ (that is, elements on the anti-diagonal line is 1 and other elements are 0), and $0_{K\times L}$ is a $K \times L$ zero matrix. For the network with multiple symmetries shown in Fig. 2 (c), its two permutation transformation matrices can be described by:

$$T_1 = \begin{pmatrix} 0 & 1 & 0 & 0 & 0 \\ 1 & 0 & 0 & 0 & 0 \\ 0 & 0 & 0 & 0 & 1 \\ 0 & 0 & 0 & 0 & 1 \\ 0 & 0 & 0 & 1 & 0 \end{pmatrix}, \quad T_2 = \begin{pmatrix} 0 & 0 & 0 & 1 & 0 \\ 0 & 0 & 0 & 0 & 1 \\ 0 & 0 & 1 & 0 & 0 \\ 1 & 0 & 0 & 0 & 0 \\ 0 & 1 & 0 & 0 & 0 \end{pmatrix} \tag{11}$$

Furthermore, if a network C has a symmetry under the transformation T, then the eigenvector matrix S of T can be described by

$$TS = S\Lambda \tag{12}$$

or

$$ST^{-1}S^{-1} = \Lambda^{-1} \tag{13}$$

where Λ is the eigenvalue matrix of T. If we denote the S-transformed adjacency matrix by M:

$$M = SCS^{-1} \tag{14}$$

then

$$M = STS^{-1}SCS^{-1}ST^{-1}S^{-1} \tag{15}$$

By inserting Eq. (13) into Eq. (15), one may find that

$$M = \Lambda M \Lambda^{-1} \tag{16}$$

i.e., the matrix M is invariant under the transformation of Λ. Thus, as long as M and Λ can be divided into four blocks:

$$M = \begin{pmatrix} a & b \\ c & d \end{pmatrix}, \quad \Lambda = \begin{pmatrix} \alpha & 0 \\ 0 & \beta \end{pmatrix} \tag{17}$$

then one has

$$\Lambda M \Lambda^{-1} = \begin{pmatrix} \alpha & 0 \\ 0 & \beta \end{pmatrix}\begin{pmatrix} a & b \\ c & d \end{pmatrix}\begin{pmatrix} \alpha^{-1} & 0 \\ 0 & \beta^{-1} \end{pmatrix}$$

$$= \begin{pmatrix} \alpha & b\alpha\beta^{-1} \\ c\beta\alpha^{-1} & \beta \end{pmatrix} \tag{18}$$

By substituting Eq. (18) into Eq. (16), we have

$$b\alpha\beta^{-1} = b, \quad c\beta\alpha^{-1} = c \tag{19}$$

These two identities hold when

$$b = c = 0 \tag{20}$$

or

$$\alpha = \beta \tag{21}$$

Note that Λ is the eigenvalue matrix of T, Eq. (20) can always be satisfied. This implies an important consequence that M is always block diagonized. Therefore, the adjacent matrix C of a network can always be block diagonized by the eigenvectors matrix of its symmetry matrix T:

$$G = S^{-1}CS = \begin{pmatrix} A & 0 \\ 0 & B \end{pmatrix} \tag{22}$$

Here A, B are two block matrices. Obviously, S is a similarity transformation, which does not change the eigenvalues of the matrix C. It only redistributes them to two blocks A and B. We denote $\{\lambda_i^{im}\}$ $(i = 1, 2, 3, \cdots, N_A)$ and $\{\lambda_i^{tv}\}$ $(i = 1, 2, 3, \cdots, N_B)$ as the eigenvalues of the two blocks, respectively, where N_A and N_B are the dimensions of matrices A and B, and $N_A + N_B = N$. Since the eigenvalue 0 must belong to one of the two blocks, we can set $\lambda_1^{im} = 0$.

3.3 The emergence of partial synchronization: the criterion

By using the above transformation which can be denoted by:

$$\boldsymbol{W} = (\Gamma \otimes S)\boldsymbol{X} \tag{23}$$

and considering that we are only concerned with the dynamics near the PaS manifold, the system Eq. (2) can be divided into two parts by only considering the leading terms. They can be written as follows respectively:

$$\dot{\boldsymbol{W}}_{im} = \boldsymbol{F}_s(\boldsymbol{W}_{im}) + \varepsilon\, \Gamma \otimes A\boldsymbol{W}_{im} \tag{24}$$

$$\dot{\boldsymbol{W}}_{tv} = \boldsymbol{F}_s(\boldsymbol{W}) + \varepsilon\, \Gamma \otimes B\boldsymbol{W}_{tv} \tag{25}$$

where $\boldsymbol{W} = (\boldsymbol{w}^1, \boldsymbol{w}^2, \cdots, \boldsymbol{w}^N) = (\boldsymbol{W}_{im}, \boldsymbol{W}_{tv})$, and $\boldsymbol{W}_{im} = (\boldsymbol{w}^1, \boldsymbol{w}^2, \cdots, \boldsymbol{w}^{N_A})$ describes the dynamics on the synchronous manifold, $\boldsymbol{W}_{tv} = (\boldsymbol{w}^{N_A+1}, \boldsymbol{w}^{N_A+2}, \cdots, \boldsymbol{w}^N)$ describes the dynamics on the transversal manifold. $\boldsymbol{F}_s$ is the function transformed from $\boldsymbol{F}$ by S.

Noticing that Eq. (24) is an independent subsystem, one can use the same method as Eq. (6) and Eq. (7) to discuss its CS problem. That is, one can linearize Eq. (24) in the vicinity of the synchronous manifold

$$\boldsymbol{w}^1 = \boldsymbol{w}^2 = \cdots = \boldsymbol{w}^{N_A} = \boldsymbol{w} \tag{26}$$

which is sub-manifold of the synchronous manifold (5). The stability of (26) can be analyzed by inserting the perturbed solution $\boldsymbol{w}^i(t) = \boldsymbol{w}(t) + \delta\boldsymbol{w}^i(t)$ $(i = 1, 2, \cdots, N_A)$ into Eq. (24) and linearizing it along the synchronous manifold $\boldsymbol{w}(t)$, and

then one may get

$$\delta \dot{\boldsymbol{w}}_{im} = [D\boldsymbol{F}_s(\boldsymbol{W}_{im}) + \varepsilon \Gamma \otimes A]\,\delta \boldsymbol{W}_{im} \tag{27}$$

Therefore, by diagonalizing the matrix (block) A, Eq. (27) can be decomposed into N_A independent equations:

$$\dot{\boldsymbol{v}}_k = [D\boldsymbol{F}_s + \varepsilon \lambda_k^{im} \Gamma]\,\boldsymbol{v}_k, \quad k = 1, 2, \cdots, N_A \tag{28}$$

We can also describe these equations by a generic form:

$$\dot{\boldsymbol{v}} = [D\boldsymbol{F}_s + \alpha \Gamma]\,\boldsymbol{v} \tag{29}$$

which is similar to Eq. (8). Moreover, the parameters that can make (26) stable are also in the regime where the largest Lyapunov exponent of Eq. (29) is negative on the α plane. When the coupling strength ε is increased to make all $\{\varepsilon\lambda_i^{im}\}$ ($i = 2, 3, \cdots, N_A$) fall into the stable regime on the α plane, the synchronous manifold (26) will be stable. Since λ_2^{im} is the last one to fall into the stable regime, it should be a criterion in judging the stability of the solution of Eq. (24) (i.e., the linear stability of the synchronous manifold).

One also can linearize Eq. (25) as:

$$\delta \dot{\boldsymbol{W}}_{tv} = [D\boldsymbol{F}_s(\boldsymbol{W}) + \varepsilon \Gamma \otimes B]\,\delta \boldsymbol{W}_{tv} \tag{30}$$

When the coupling strength is increased, all $\{\varepsilon\lambda_i^{tv}\}$ ($i = 1, 2, 3, \cdots, N_B$) fall into the stability regime in the α plane, implying the stability of Eq. (25) and λ_1^{tv} is the last one falling into the stability regime. On the other hand, because Eq. (25) describes the transversal subsystem, its stability (its largest Lyapunov exponent is negative) suggests the stability of the PaS manifold (4) of the whole system, i.e., the emergence of PaS. If $\lambda_2^{im} < \lambda_1^{tv}$, then the coupling strength that makes $\varepsilon\lambda_2^{im}$ falling into the stability regime will be smaller than that of $\varepsilon\lambda_1^{tv}$. Therefore, the synchronization of Eq. (24) will be achieved at a smaller coupling than that for Eq. (25), thus a global synchronization state has been achieved when Eq. (25) is stable, i.e., the PaS state can not be observed. Therefore the emergence of PaS requires:

$$\lambda_2^{im} > \lambda_1^{tv} \tag{31}$$

By noticing that $\{\lambda_i^{im}\}$ and $\{\lambda_j^{im}\}$ are all eigenvalues of the adjacent matrix C (or more precisely, eigenvalues of the two block matrices A and B, respectively), the above inequality indicates that the largest eigenvalue of the transversal manifold should be less than the second largest eigenvalue of the PaS manifold. This criterion is very interesting that it relates to λ_2^{im}, which is very significant as compared with the criterion of global synchronization that $\lambda_1^{tv} < \lambda_1^{im} = 0$.

Now let us briefly summarize the procedure to judge whether PaS can emerge on a given network:

(1) Analysis of the topological symmetry of the network: If no topological symmetry exists, the PaS can not be achieved on this network;

(2) Diagonalization of the adjacent matrix of the network by using the eigenvector matrix of the symmetry matrix;

(3) Comparison of the eigenvalues of the two blocks: If eigenvalues satisfy the inequality (31), then the PaS state should be stable;

(4) By increasing the coupling strength ε, when $\varepsilon\lambda_1^{tv}$ falls into the stable regime, the PaS can be observed, and this value $\varepsilon_{\mathrm{PaS}}$ is the critical coupling of PaS.

We must stress that this criterion is generic. Throughout the above discussions, we did not require the form of the topology of the matrix. Moreover, we did not limit the symmetry of the network, and thus the criterion for the emergence of PaS states should not be limited to networks with mirror symmetries. It should also be noted that the above criterion is irrelevant to the specific dynamics on nodes. Therefore, PaS patterns are closely related to the symmetry of the network topology.

4 Partial synchronization: numerical experiments

Now we continue to perform our numerical simulations to discuss the PaS patterns. As we will see, the stability and furthermore the emergence of the above observed rich PaS patterns can be well studied in a more insightful way in terms of the theoretical criterion we proposed above. Furthermore, one may potentially predict the emergence of PaS patterns by using the criterion, including the case of multiple topological symmetries and the interesting PaS pattern competitions and selection.

For simplicity, we still limit our discussions on the representative case of ring-type networks with small numbers of shortcuts. As we showed in the previous section on numerical simulations, PaS can always be achieved on regular networks with one shortcut. To test the validity of the above criterion, we take the ring network with $N_s = 2$ as an example.

4.1 PaS on ring networks with two shortcuts

For a systematic analysis, it is necessary to find all possible networks satisfying the mirror symmetry. For two non-local couplings, one has four ends. For convenience, we always take the node $i = 1$ as one of the ends. The second and the third ends are labelled as j and k ($k > j$), respectively. Due to the mirror symmetry, the label of the fourth end is $n_4 = k + j - 1$. The ring network satisfies the translational symmetry, i.e., the dynamical property keeps invariant under the transformation $i \to i + i_0$ for any $i_o \in [1, N]$. Therefore one has $2 \leqslant j \leqslant N/2$ and $j \leqslant k \leqslant N/2$. In terms of this labelling rule, one may find three possible links that hold the mirror symmetry:

(1) The *parallel network* (PN) refers to a network with two non-local couplings denoted by $(1, n_4)$ and (j, k), which are parallel to each other, as shown in Fig. 5 (a);

(2) The so-called *cross network* (CN) refers to a network

with two crossed non-local couplings labelled by (1, k) and (j, n_4), as shown in Fig. 6 (a);

(3) The "*lambda*" *network* (LN) is named as a network with two non-local λ-shaped couplings (1, j) and (k, n_4), as shown in Fig. 7 (a).

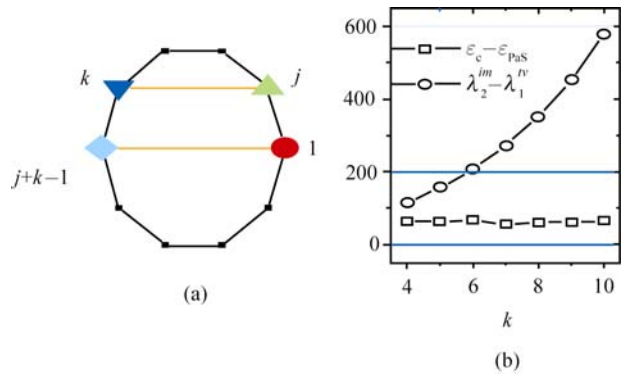

Fig. 5 Parallel network. **(a)** The label rule for a parallel network with $N_s = 2$. **(b)** The comparison between $\varepsilon_c - \varepsilon_{PaS}$ and $\lambda_2^{im} - \lambda_1^{tv}$, $N = 20$, $j = 3$. $\lambda_2^{im} - \lambda_1^{tv}$ has a magnification of 10^3.

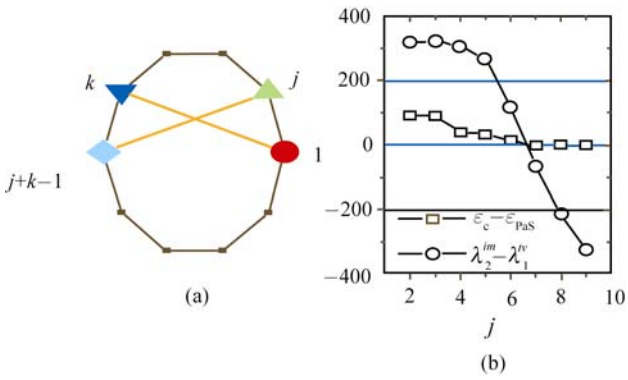

Fig. 6 Cross network. **(a)** The label rule for a cross network with $N_s = 2$. **(b)** The comparison between $\varepsilon_c - \varepsilon_{PaS}$ and $\lambda_2^{im} - \lambda_1^{tv}$, $N = 20$, $k = 9$. $\lambda_2^{im} - \lambda_1^{tv}$ has a magnification of 10^3.

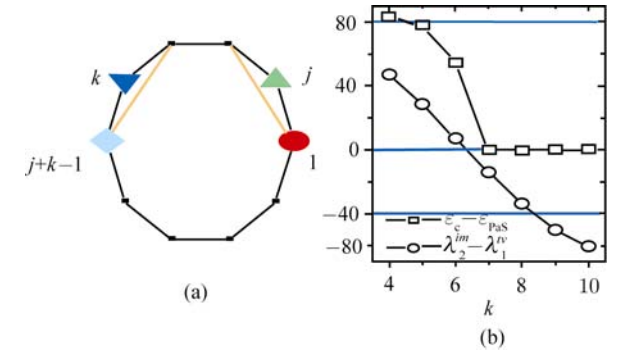

Fig. 7 Lambda network. **(a)** The label rule for a lambda network with $N_s = 2$. **(b)** The comparison between $\varepsilon_c - \varepsilon_{PaS}$ and $\lambda_2^{im} - \lambda_1^{tv}$, $N = 20$, $j = 3$. $\lambda_2^{im} - \lambda_1^{tv}$ has a magnification of 10^3.

Thus by varying j and k, all symmetric networks with two non-local couplings can be found.

In the following numerical experiments, we still use the Lorenz oscillator as the nodes of the network (the equations of motion, parameters and Γ are same as that in Section 2). As we have shown in Section 2, the same results can be achieved if one use other types of oscillators as the nodes or other types of coupling schemes as links.

We find in numerical experiments that the PaS state can always be observed for PN's. For CN and LN, PaS can only be observed for some of these network configurations, i.e., PaS cannot be observed on some CN's and LN's. Let us discuss the ring of $N = 20$ Lorenz oscillators with $N_s = 2$ nonlocal couplings. We denote ε_c as the critical coupling of CS of the whole system and ε_{PaS} as the critical coupling of PaS (the coupling strength that the oscillators which are symmetric with each other become synchronous). One further introduces the difference $\Delta\varepsilon = \varepsilon_c - \varepsilon_{PaS}$ to measure threshold difference between CS and PaS. If $\Delta\varepsilon > 0$, then the emergence of PaS is earlier than that of CS, i.e., PaS can be first observed as one increases the coupling strength ε. On the contrary, $\Delta\varepsilon = 0$ implies that PaS and CS are achieved at the same critical coupling, i.e., PaS can't be observed. To observe whether the PaS can be achieved (stabilized), it is convenient to introduce the difference between two eigenvalues λ_2^{im} and λ_1^{tv}, $\Delta\lambda = \lambda_2^{im} - \lambda_1^{tv}$. Based on the criterion of PaS given in Eq. (31), the PaS state corresponds to the regime where $\Delta\lambda > 0$.

In Figs. 5 (b), 6 (b) and 7 (b), the two differences $\Delta\lambda$ and $\Delta\varepsilon$ against k (or j) are shown by fixing j (or k) for PN's, CN's, and LN's, respectively. For PN's shown in Fig. 5 (a), it can be found from Fig. 5 (b) that $\Delta\varepsilon$ is always larger than 0, indicating that PaS can always be observed on this kind of networks. It is interesting that $\Delta\lambda > 0$ for all k, implying that the PaS state is always a stable solution of the PN, which coincides perfectly well with the result of $\Delta\varepsilon > 0$. Figure 6 (b) and Fig. 7 (b) present the comparison between $\Delta\lambda$ and $\Delta\varepsilon$ for cross and lambda networks. The agreement between the PaS regime given by positive $\Delta\varepsilon$ and that given by positive $\Delta\lambda$ is perfectly good. Moreover, not all CN's and LN's possess the stable PaS state, i.e., for some configurations of networks PaS cannot be observed. For CN's, the PaS state is more stable if two shortcuts are farther from the symmetry axis; while for LN's the PaS state is unstable if two nonlocal links are apart from each other. For example, as shown in Fig. 6 (b) [cross network], for $k = 9$, PaS emerges when $j < 7$. For the LN shown in Fig. 7 (b), as $j = 3$, PaS can be observed when $k < 7$.

As indicated above, PaS states can be observed only on some CN's and LN's. A natural question may arise: Does the above conclusion depend on node numbers of networks ? We may discuss the PaS phase diagram in the re-scaled plane (j/(N/2), k/(N/2)), where the critical lines separating the synchronous and asynchronous states are given in Fig. 8

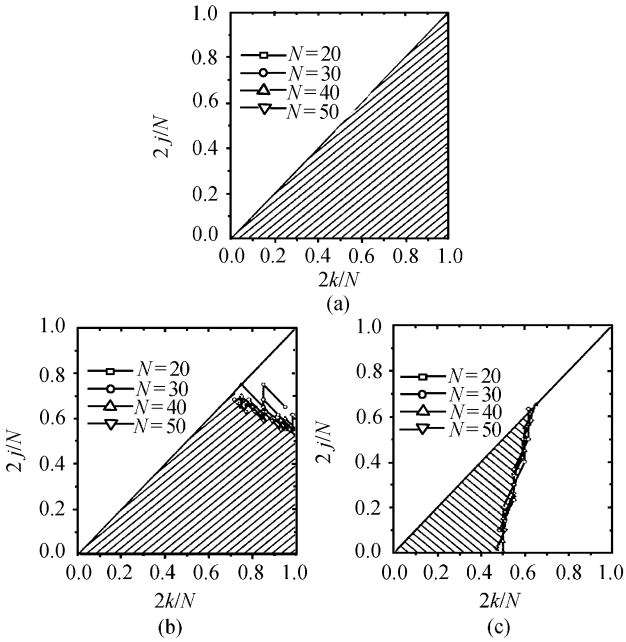

Fig.8 The PaS regimes (labelled by sparse lines). **(a)** Parallel network; **(b)** Cross network; **(c)** Lambda network.

5 Synchronization of sparsely coupled spatiotemporal systems: an application

The theoretical criterion we proposed in fact can be naturally applied to the studies of the synchronization between two spatiotemporal systems. Let us consider a network composed of two identical groups. Each group is simply a chain of N chaotic oscillators (here we use the Rossler oscillators) with nearest-neighbor couplings (here we use the intragroup y-coupling with the strength ε). Between two groups, there are only a few (sparse) connections with intergroup coupling strength r).

As shown in Figs. 9 (a) and (b), L_1 and L_2 are the connections between groups. We are interested in the synchronization between these two groups when only a few intergroup connections are considered. When all the corresponding elements in two groups are synchronized to each other, we call this behavior the *group synchronization* (GrS). Generally, each group has N nodes, and between two groups there are n_l connections named $L_1, L_2, \cdots, L_{n_l}$. For example, we have L_1=1 if the first pair of oscillators is coupled to each other.

Let us analyze the possibility of GrS in terms of the above method on PaS. In fact, we can regard the two groups as one system with $2N$ nodes. Obviously the topology of this system satisfies the mirror symmetry. Then the system can be divided into two parts: $\boldsymbol{G}_l = \boldsymbol{X} + \boldsymbol{X}'$ and $\boldsymbol{G}_r = \boldsymbol{X} - \boldsymbol{X}'$, where $\boldsymbol{G}_l = (\boldsymbol{g}_l^1, \boldsymbol{g}_l^2, \cdots, \boldsymbol{g}_l^N)$ and $\boldsymbol{G}_r = (\boldsymbol{g}_r^1, \boldsymbol{g}_r^2, \cdots, \boldsymbol{g}_r^N)$ describes the dynamics of the *globally synchronous* (GlS) manifold and that of the GrS manifold, respectively. We only care about the dynamics near the synchronous states, then the system can be linearized as:

$$\delta \boldsymbol{G}_l = [D\boldsymbol{F}(\boldsymbol{F}_l) + \Gamma \otimes A]\,\delta \boldsymbol{G}_l \tag{32}$$

$$\delta \dot{\boldsymbol{G}}_r = [D\boldsymbol{F}(\boldsymbol{G}_r) + \Gamma \otimes B]\,\delta \boldsymbol{G}_r \tag{33}$$

where

$$[\Gamma \otimes A(\delta \boldsymbol{G}_l)]^i = \varepsilon \Gamma(\delta G_l^{i+1} + \delta G_l^{i-1} - 2\delta G_l^i) \tag{34}$$

where $i = 1, 2, \cdots, N$, and

$$[\Gamma \otimes B(\delta \boldsymbol{G}_r)]^i = \varepsilon \Gamma(\delta G_r^{i+1} + \delta G_r^{i-1} - 2\delta G_r^i) \tag{35}$$

for oscillators without intergroup couplings. For those coupled pairs, one has

$$[\Gamma \otimes B(\delta \boldsymbol{G}_r)]^j = \varepsilon \Gamma(\delta G_r^{j+1} + \delta G_r^{j-1} - 2\delta G_r^j) - 2r\Gamma\delta G_r^j \tag{36}$$

The GrS should occur before the emergence of GlS. Therefore the GrS requires $\lambda_2^l > \lambda_1^r$.

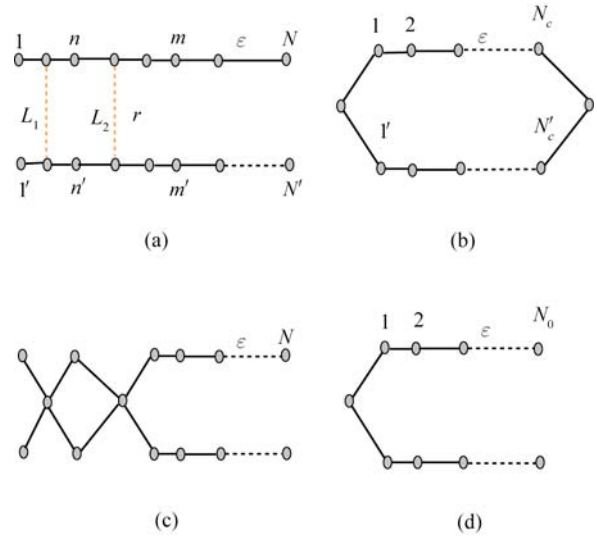

Fig. 9 **(a)** Two sparsely coupled chains. **(b)** Two sparsely coupled circles; **(c)** Strong-coupling limit of two coupled chains. **(d)** Two intergroup coupled oscillators can be considered as a single one. **(e)** The closed loop structure. **(f)** The open block structure.

In fact, the structural properties of a network have great affects on the GrS behavior. Some topology structure could satisfy $\lambda_2^l > \lambda_1^r$ and GrS could occur. However, some topology structures could never satisfy $\lambda_2^l > \lambda_1^r$ and never achieve GrS with any intergroup coupling strength r. So we analyze the topology structure of the whole system. By studying connections between groups in an asymptotic regime, namely at strong-coupling limit ($r = \infty$), as shown in Fig. 9 (c). In this regime, the coupled oscillators can be regarded as a common oscillator for two groups in Fig. 9 (d). Therefore the coupled system is divided into three parts with two types of topological structures: the closed block shown in Fig. 9 (e) and the open block given in Fig. 9 (f). The eigenvalues for the

GlS manifold can be worked out as:

$$\lambda_q^l = -4\varepsilon \sin^2(q/2) \tag{37}$$

where $q = m\pi/N$, $m = 0, 1, 2, \cdots, N-1$. The eigenvalues for the GrS manifold of the closed block are

$$\lambda_q^r = -4\varepsilon \sin^2(q/2) \tag{38}$$

where $q = m\pi/(N_c+1)$, and $m = 1, 2, \cdots, N_c$. The eigenvalues for the GrS manifold of the open block are

$$\lambda_q^r = -4\varepsilon \sin^2(q/2) \tag{39}$$

where $q = (2m-1)\pi/(2N_o+1)$, and $m = 1, 2, \cdots, N_o$. If there are n_l connected pairs between two groups, the system will be divided into n_o open blocks and n_c closed blocks. Obviously $n_o + n_c - 1 = n_l$, and $\sum^{n_o} N_o + \sum^{n_c} N_c + n_l = N$. According to the analysis of the eigenvalues, one should find some useful results:

- The larger the size of a block is, the larger λ_1^r is, and the more difficult for $\lambda_2^l > \lambda_1^r$. Therefore GrS becomes difficult if the size of the block in the network is very large.
- If there is an open block with the size $n \geqslant N/2$ (half size of the system), GrS cannot be achieved before GlS, i.e., GrS cannot be observed.
- An open bloc with size n has the same eigenvalue and the same synchronization ability as a close block with size $2n$.
- The optimal connection way in achieving GrS for two groups can be theoretically predicted. The least number of intergroup connections is two, and the optimal way of two connections should form two open blocks with the size $n = (N-2)/4$ and one closed block with the size $(N-2)/2$.

For two connected circle-structure groups with n_l connections, only n_c closed blocks with size N_c exist at infinite-connection limit ($r = \infty$) with $\sum^{n_c} N_c + n_l = N$. The eigenvalues for the GlS manifold can be solved as:

$$\lambda_q^l = -4\varepsilon \sin^2(q/2) \tag{40}$$

where $q = 2m\pi/N$, and $m = 0, 1, 2, \cdots, N-1$. The eigenvalues for the GrS manifold of the closed blocks are

$$\lambda_q^r = -4\varepsilon \sin^2(q/2) \tag{41}$$

where $q = m\pi/(N_c+1)$, and $m = 1, 2, \cdots, N_c$. If there are two connections between two circle-structure groups, the optimal way is to divide the system into two closed blocks with the same size and $2N_c = N-2$, $\lambda_2^l = \lambda_1^r$. Therefore, for circle-structure groups, the least number of intergroup connections for GrS is three.

We carried out numerical simulations to study the synchronization between two groups of coupled oscillators. In Fig. 10 (a) for two coupled circle networks with $N = 8$ and two intergroup links $L_1 = 2$ and $L_2 = 6$, the system can be divided into two closed blocks with $N_c = 3$, and $\lambda_2^l / \lambda_1^r = 1$. GrS can not be achieved before GlS. In Fig. 10 (b) for two coupled chain networks with $N = 23$ and three intergroup links $L_1 = 5$, $L_2 = 13$ and $L_3 = 19$, the system has no open blocks with $N_o > N/2$ and then GrS occur. For example, for the networks shown in Fig. 10 (c) with two coupled $N = 18$ chains, we choose different ways of connections. When $L_1 = 5$, $L_2 = 14$ (the optimal connection with one closed bloc which size is 8, and two open blocs which sizes are both 4), the smaller coupling is needed to achieve GrS. In Fig. 10 (d), we draw the $\varepsilon - r$ phase space for the real network of two coupled $N = 10$ chains with $L_1 = 3$ and $L_2 = 8$. The phase space is divided into five parts: the unsynchronized state (US), the state of synchronization between groups (GrS), the state of synchronization inside the individual group (IS), the state of complete synchronization (CS) and the transition state as shown in the small green area. The blue dot arrows in Fig. 10 (d) exhibit the different paths to complete synchronization. An unsynchronized system is capable of choosing various ways to complete synchronization through GrS, IS or the transition state. This suggests a phase-transition-like phenomenon.

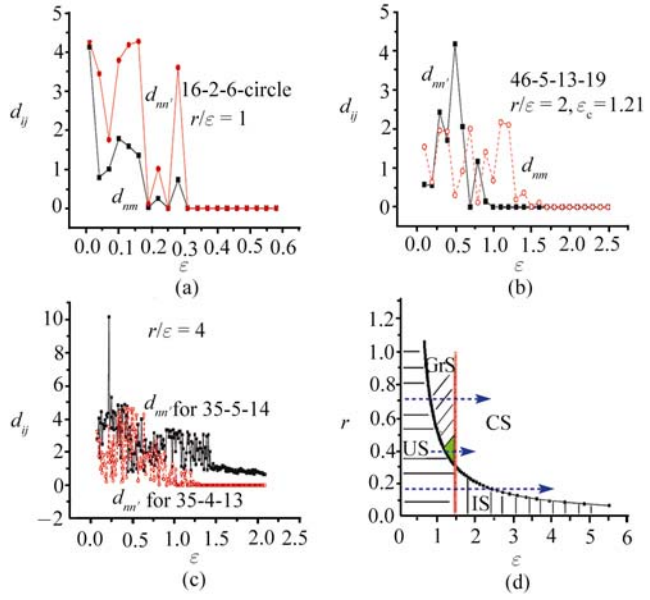

Fig. 10 **(a), (b), (c)** Trajectory distances of intergroup and intragroup oscillators; **(d)** Synchronization phase diagram.

6 Conclusions

In conclusion, in this paper we explored the interesting partial synchronization dynamics induced by breaking the topological symmetry of the networks and the synchronization of spatiotemporal systems. A method and an analytical criterion in judging the stability of PaS state on a given network are proposed in terms of a comparison between the LES of the PaS manifold and that of the transversal mani-

fold. This criterion is verified in numerical simulations. The criterion we proposed in this paper is valid as long as the symmetry property of the network is known and the corresponding PaS solution can be determined. We apply the criterion of PaS to the explorations of synchronization of sparsely coupled spatiotemporal systems. We find that different topologies of intergroup couplings may lead to different synchronizability. The analytical treatment reveal the transitions of synchronous regimes.

The present studies reveal the intrinsic collective bifurcation of coupled dynamical systems prior to the emergence of global synchronization. The phenomena we revealed and the theoretical discussions we proposed in this paper should be potentially significant in revealing the pattern dynamics in spatiotemporal systems [45]. We hope that the present studies can shed light on some currently intriguing problems such as synchronization dynamics, pattern dynamics, and network dynamics.

Acknowledgements This work was supported in part by the key National Natural Science Foundation of China, the Foundation for the Author of National Excellent Doctoral Dissertation of China, the Teaching and Research Award Program for Outstanding Young Teachers in Higher Education Institutions of Ministry of Education, and the Foundation of Doctoral Training.

References

1. Pecora L. M. and Carroll T. L., Phys. Rev. Lett., 1990, 64: 821
2. Pikovsky A., Rosenblum M., and Kurths J., Synchronization: A universal concept in nonlinear sciences, Cambridge University Press, Cambridge, 2001
3. Boccaletti S., Grebogi C., Lai Y. C., Mancini H., and Maza D., Phys. Rep., 2000, 329: 103
4. Boccaletti S., Kurths J., Osipov G., Valladares D. L., and Zhou C. S., Phys. Rep., 2002, 366: 1
5. Timme M., Wolf F., and Geisel T., Phys. Rev. Lett., 2004, 92: 074101
6. Hunt B. R., Ott E., and Yorke J. A., Phys. Rev. E, 1997, 55(4): 4029
7. Liu Z. H. and Chen S. G., Phys. Rev. E, 1997, 56: 7297
8. Zheng Z. G., Wang X. G., and Cross M. C., Phys. Rev. E, 2002, 65(5): 056211
9. Rosenblum M., Pikovsky A., and Kurths J., Phys. Rev. Lett., 1996, 76: 1804
10. Osipov G., Pikovsky A., Rosenblum M., and Kurths J., Phys. Rev. E, 1997, 55(3): 2353
11. Parlitz U., Junge L., and Kocarev L., Phys. Rev. E, 1996, 54: 2115
12. Rosenblum M. G. Pikovsky A. S., and Kurths J., Phys. Rev. Lett., 1996, 76: 1804
13. Zheng Z., Hu G., and Hu B., Phys. Rev. Lett., 1998, 81: 5318
14. Ernst et al., Phys. Rev. Lett., 1995, 74: 1570
15. Hu G., et al., Phys. Rev. Lett., 2000, 85: 3377
16. Parekh N., Parthasarathy S., and Sinha S., Phys. Rev. Lett., 1998, 81: 1401
17. Watts D. J. and Strogatz S. H., Nature (London), 1998, 393: 440
18. Strogatz S. H., Nature, 2001, 410: 268
19. Albert R. and Barabasi A. L., Rev. Mod. Phys., 2002, 74: 47
20. Newman M. E. J., SIAM Rev., 2003, 45: 167
21. Jalan S. and Amritkar R. E., Phys. Rev. Lett., 2003, 90: 014101
22. Hwang D. -U., Chavez M., et al., Phys. Rev. Lett., 2005, 94: 138701
23. Chavez M., Hwang D. -U., et al., Phys. Rev. Lett., 2005, 94: 218701
24. Newman M. E. J., et al., Phys. Rev. Lett., 2000, 84: 3201
25. Lago- Fernandez L. F., et al., Phys. Rev. Lett., 2000, 84: 2758
26. Barahona M. and Pecora L. M., Phys. Rev. Lett., 2002, 89: 054101
27. Wei G. W., et al., Phys. Rev. Lett., 2002, 89: 284103
28. Nishikawa T., et al., Phys. Rev. Lett., 2003, 91: 014101
29. Atay F. M., et al., Phys. Rev. Lett., 2004, 92: 144101
30. Jiang Y., et al., Phys. Rev. E, 2003, 68: 065201(R)
31. Restrepo J. G., et al., Phys. Rev. E, 2004, 69: 066215
32. Moreno Y. and Pacheco A. F., Europhys. Lett., 2004, 68: 603
33. Yonker S., et al., Phys. Rev. E, 2006, 73: 026218
34. Gray C. M., Koenig P., Engel A. K., and Singer W., Nature (London), 1989, 338: 334
35. Pyragas K., Phys. Rev. E, 1996, 54: R4508
36. Stewart I., Golubitsky M., and Pivato M., SIAM J. Applied Dynamical Systems, 2003, 2(4): 609
37. Ao Bin and Zheng Z., Europhys. Lett., 2006, 74: 229
38. Ao Bin and Zheng Z., Phys. Rev. E, 2006 (submitted)
39. Ao Bin, Ma X., Li Y., and Zheng Z., Chin. Phys. Lett., 2006, 23: 786
40. Ao Bin, Ma X., Li X., and Zheng Z., Int. J. Mod. Phys. B, 2006 (in press)
41. Feng X., Zheng Z., and Cross M., Phys. Rev. E, 2006 (to be submitted)
42. Yang J., et al., Phys. Rev. Lett., 1998, 80: 496
43. Pecora L. M. and Carroll T. L., Phys. Rev. Lett., 1998, 80: 2109
44. Zhang Y., et al., Phys. Rev. E, 2001, 63: 026211
45. Xiao J., Li H., Yang J., and Hu G., Frontiers of Physics in China, 2006, 1(2): 204